Reminder: Semi-Conductors, I

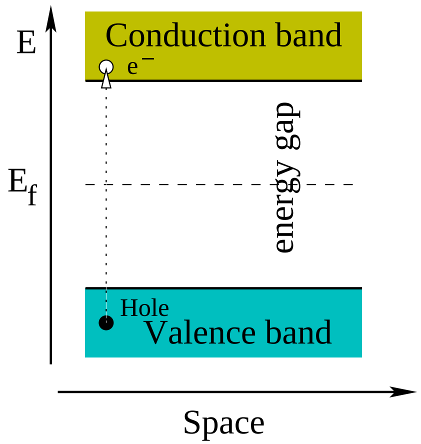

Semiconductors: separation of valence band and conduction band ~1 eV (=energy of visible light).

Absorption of photon in Si: Energy of photon released

Number of electron-hole pairs produced:

$$N \sim \frac{h\nu}{E_{\text{gap}}} \qquad (3.18)$$

in other words:

- optical light: ~1 electron-hole pair
- X-rays (keV): ~1000 electron-hole pairs

Problem: electron-hole pairs recombine immediately in a normal semiconductor.

Reminder: Semi-Conductors, II

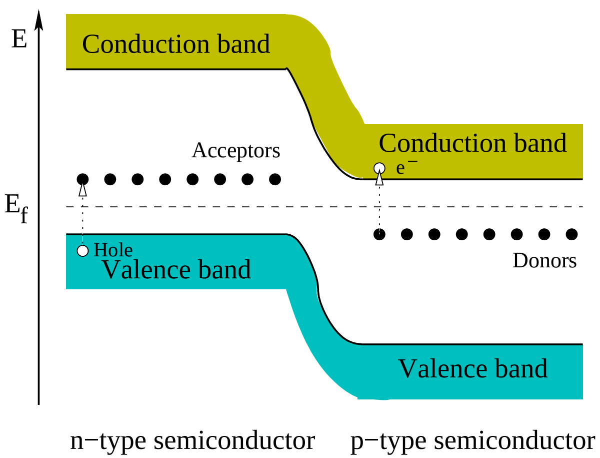

"Doping" the semiconductor moves the valence- and conduction bands.

Connecting a "n-type" and a "p-type" semiconductor gives a pn-junction.

Electron-hole pairs created at pn-junction will be separated by field gradient

$\Longrightarrow$ electrons can then be collected in potential well away from the junction and read out.

Reminder: Semi-Conductors, III

Number of electron-hole pairs produced determined by band gap + "dirt effects"

("dirt effects": e.g., energy loss going into bulk motion of the detector crystal ["phonons"])

Material	Z	Band gap (eV)	E/pair (eV)
Si	14	1.12	3.61
Ge	32	0.74	2.98
CdTe	48–52	1.47	4.43
HgI2	80–53	2.13	6.5
GaAs	31–33	1.43	5.2

(so ~1 electron for optical photons, ~1000 electrons for X-rays)

Since band gap small: thermal noise $\Longrightarrow$ need cooling

(ground based: liquid nitrogen, −200°C, in space: cryostats)

Strip Detectors

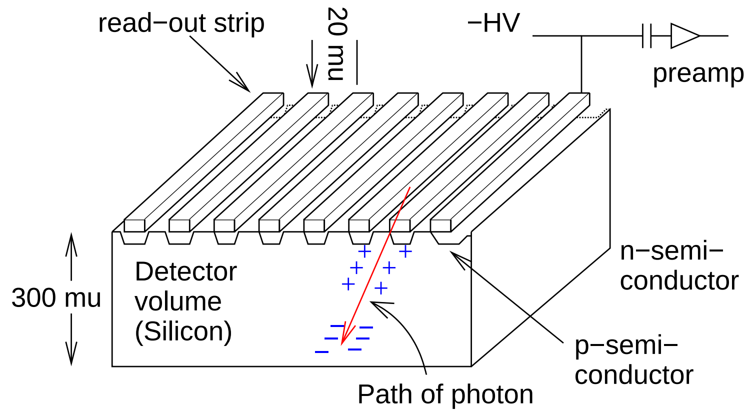

after Grupen

First attempt at spatial resolution obtained by segmenting the p-doped layer: microstrip detectors

CCDs, I

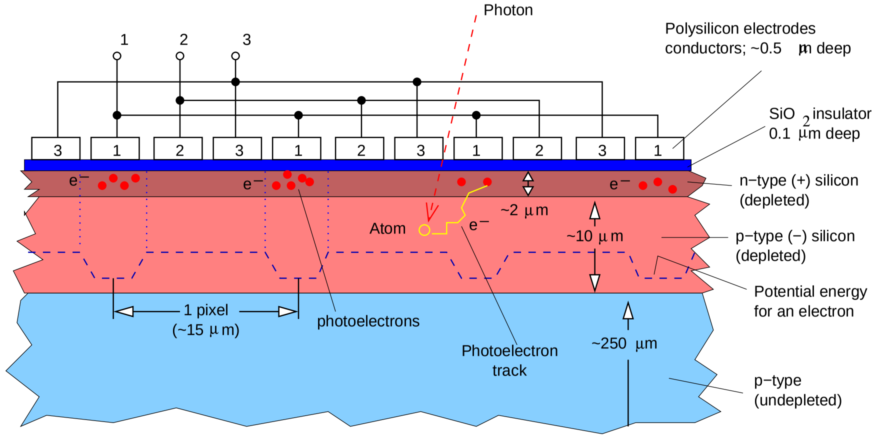

After Bradt

Two-Dimensional imaging is possible with more complicated semiconductor structures: Charge Coupled Devices (CCDs).

CCDs, II

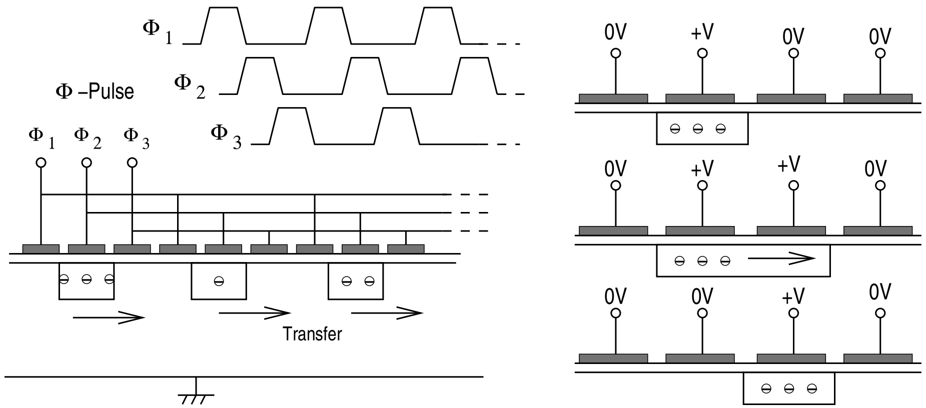

after McLean (1997, Fig. 6.9)

Principle of the readout of a CCD with Φ-pulses.

CCDs, III

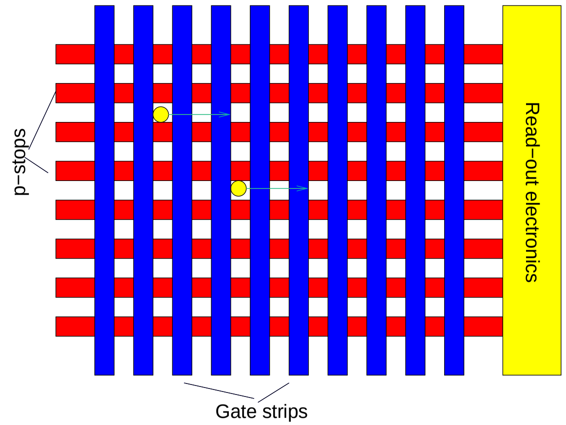

By combining several of these readout stripes one obtains a two dimensional detector.

Separation of individual columns with p-stops, highly doped Si, to prevent charge diffusion between columns.

Read out either by moving charge to one corner, preamplifying, and digitizing, or by having one amplifier and analog-digital-converter per column.

The latter is expensive, only done in the fastest X-ray CCDs.

CCDs, IV

optical CCDs: measure intensity $\Longrightarrow$ need *long* exposures

X-ray CCDs: measure individual photons $\Longrightarrow$ need fast readout

bright sources: several 1000 photons per second $\Longrightarrow$ readout in μs!

In X-rays: spectroscopy possible. Typical resolution reached today:

$$\frac{\Delta E}{E} = 2.355\sqrt{\frac{3.65\,\text{eV}\cdot F}{E}} \tag{3.19}$$

with $F \sim 0.1 \Longrightarrow \sim 0.4\%$, so much better than proportional counters.

(but same $\Delta E/E \propto E^{-1/2}$ proportionality because of Poisson!)

For both optical and X-rays: sensitivity close to 100%

Si based CCDs are currently the best available imaging photon detectors for optical and X-ray applications.

CCDs, V

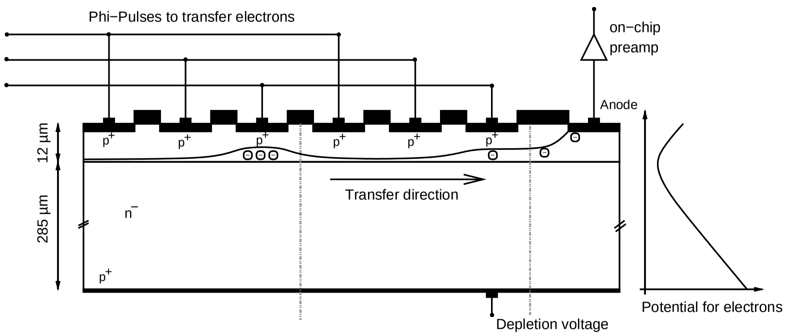

Schematic structure of the *XMM-Newton* EPIC pn CCD.

Problem: Infalling structure has to pass *through* structure on CCD surface ⟹ loss of low energy response, also danger through destruction of CCD structure by cosmic rays...

Solution: Irradiate the back side of the chip. Deplete whole CCD-volume, transport electrons to pixels via adequate electric field ("backside illuminated CCDs")

Note: solution works mainly for X-rays

XMM-Newton: EPIC-pn CCD, I

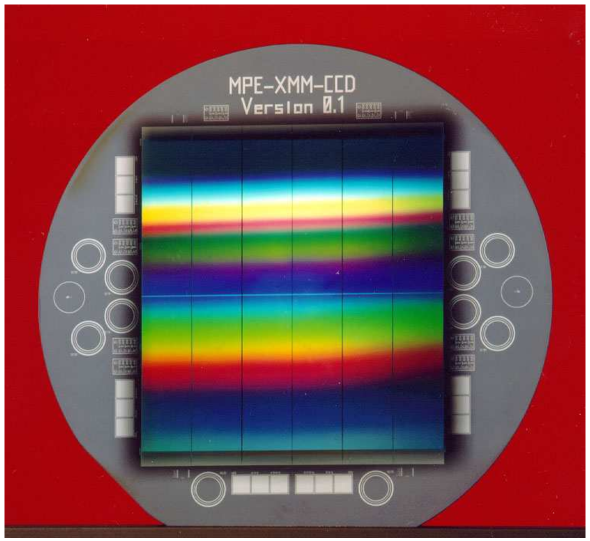

XMM-Newton: Array of individual backside illuminated CCDs on one Silicon wafer ⟹ requires extreme care during production

at the time of production one of the most complex Silicon structures ever made (diameter: 65.5 mm)

XMM-Newton: EPIC-pn CCD, II

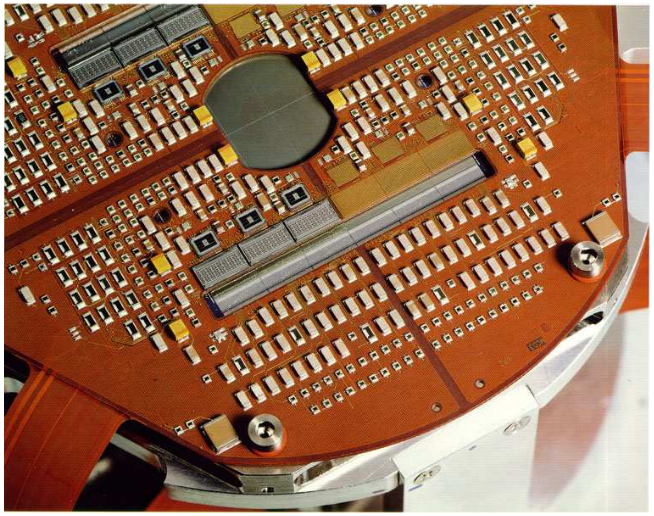

Backside of the EPIC-pn camera head

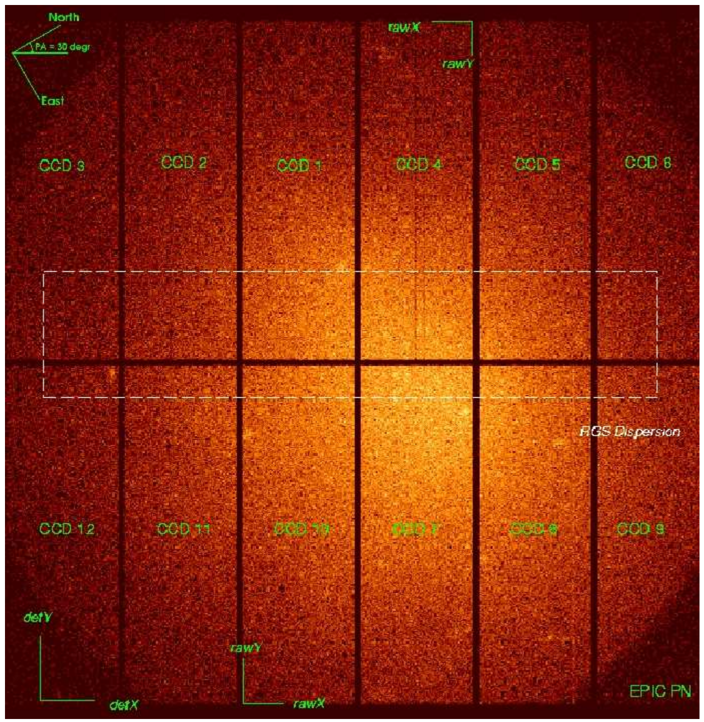

ESA

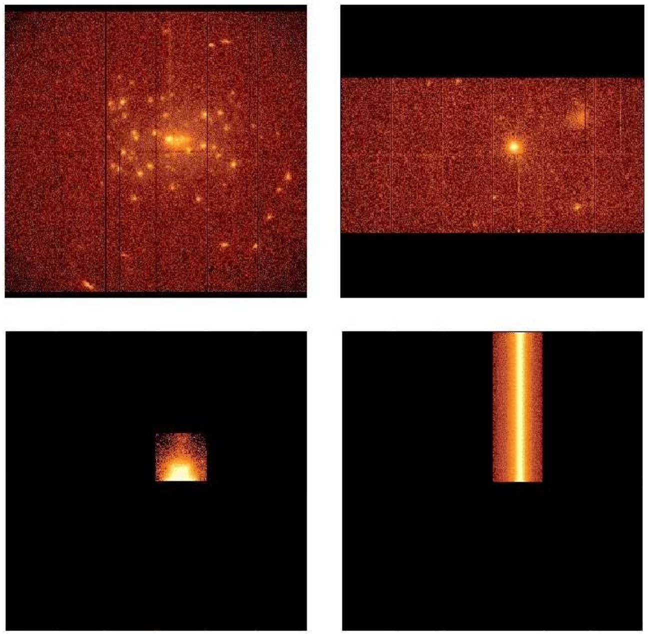

Different read out strategies can be used to speed up the read out in case bright sources are observed to allow X-ray timing and to avoid pile-up:

- Full frame mode: 376×384, $\Delta t = 73$ ms
- Large Window mode: 198×384, $\Delta t = 48$ ms
- Small Window mode: 63×64, $\Delta t = 6$ ms
- Timing Mode: 64×200, $\Delta t = 0.03$ ms
- Burst Mode: 64×180, $\Delta t = 7\,\mu$s, but only 3% efficiency

ESA

XMM-Newton: EPIC-MOS CCD, I

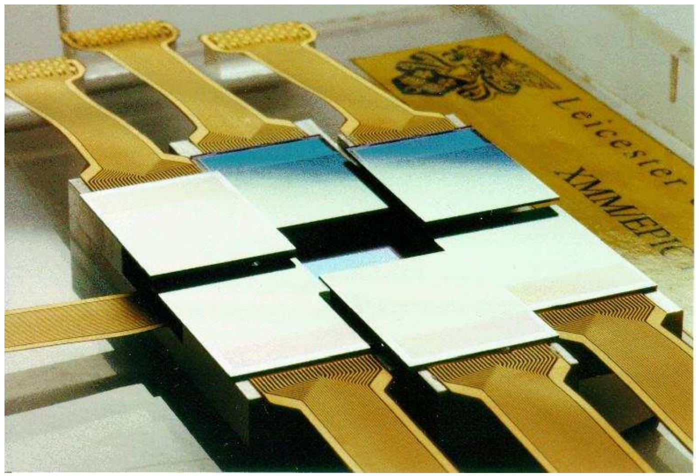

XMM-Newton (EPIC-MOS; Leicester): 7 single CCDs with 600 × 600 pixels, mounting is adapted to curved focal plane of the Wolter telescope.

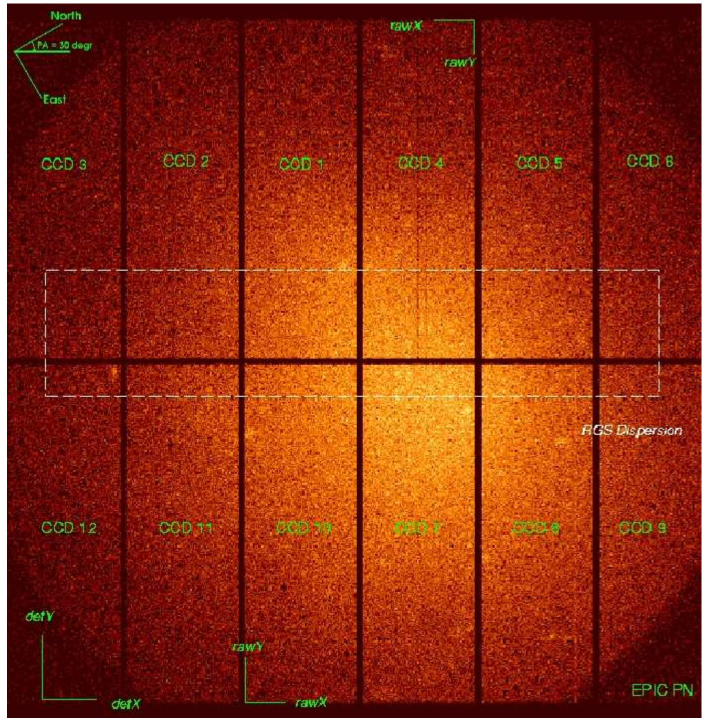

ESA

Chandra: ACIS

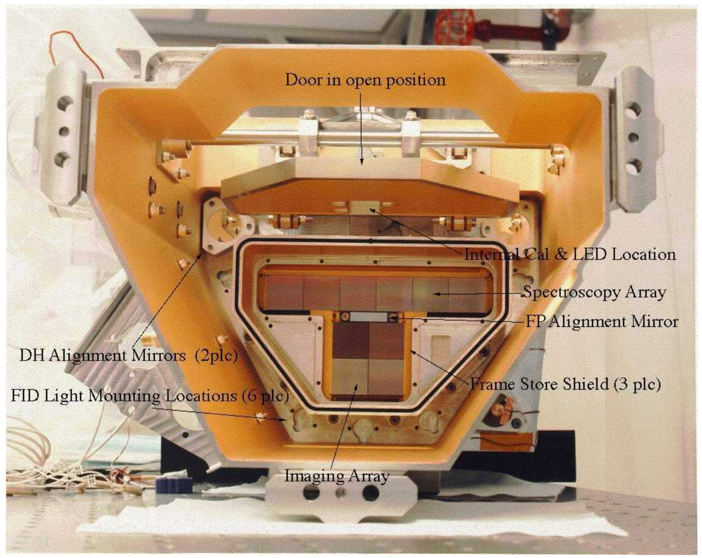

Chandra (ACIS): 10 frame store CCDs

MIT-CXC

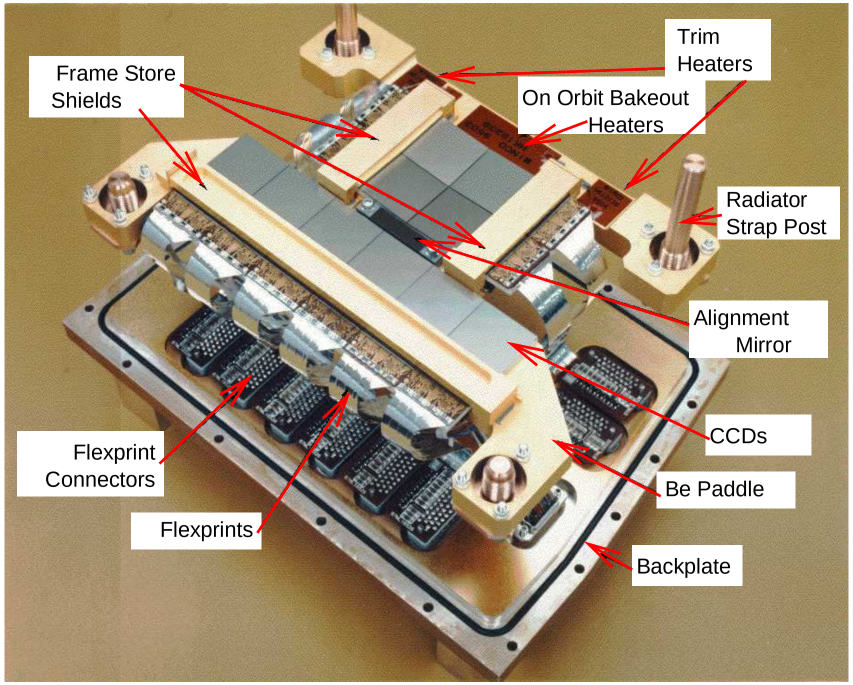

after MIT-CXC

Chandra: ACIS

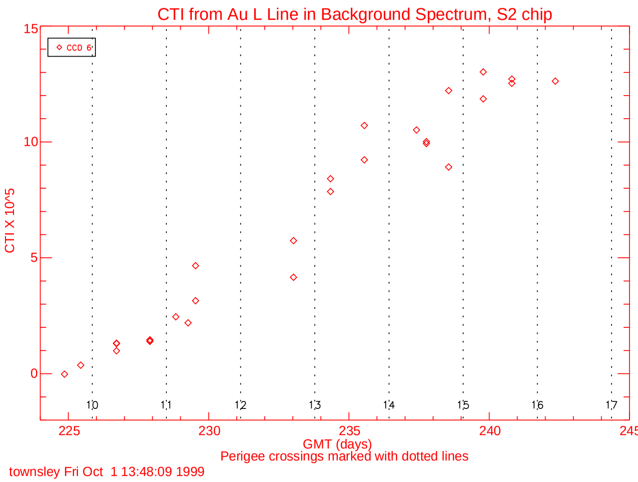

Shortly after launch in 1999 July, ACIS front illuminated CCDs showed significant increase in Charge Transfer Inefficiency (CTI).

Explanation: Low energy protons ($E < 1$ MeV) damaging gate structure of FI chips; are focused onto CCD by mirrors.

CTI: Fraction of charge lost when transporting electrons from one pixel to the next. Often also used: Charge Transfer Efficiency (CTE) (CTE $= 1 -$ CTI).

Collimators

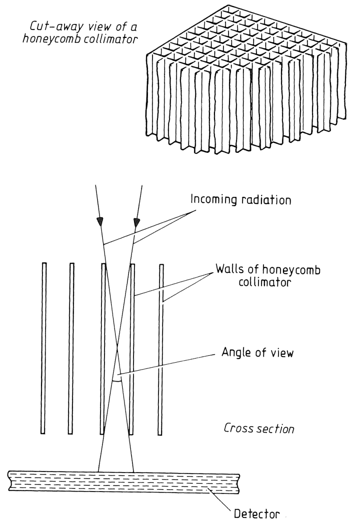

At energies above $\sim$10 keV, imaging with mirror systems is not technically possible.

Apart from multilayer-technologies, but those have not yet flown.

$\Longrightarrow$ need other ways to ensure that we only see the object we want to see.

Simplest method: honeycomb collimator, i.e., a variant of a pinhole camera.

Field of view: FOV $\sim d/h$ where d tube diameter, h tube length; typical values $\sim$degrees.

(Kitchin, Astrophysical Techniques, Fig. 1.3.5)

Coded Mask Telescopes, I

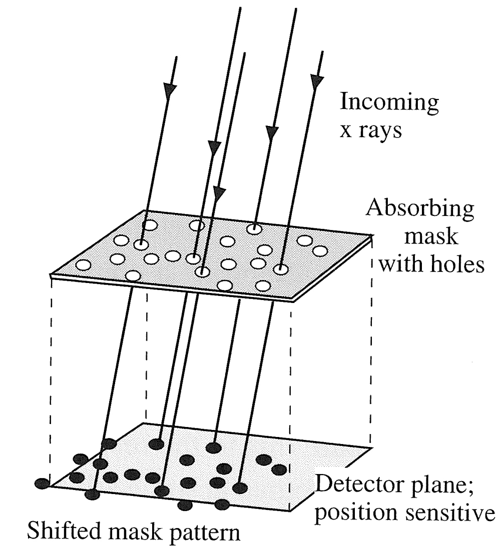

Problem of collimators: no imaging capabilities

Solution: Coded Masks

$\Longrightarrow$ Combination of mask with multiple holes and position sensitive detector.

Typically, 25% to 50% of the mask is open.

(Bradt, Fig. 5.3)

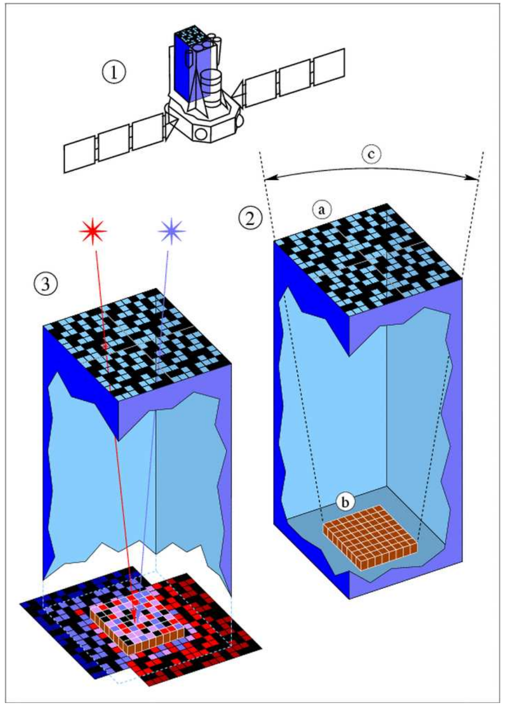

Principle of image reconstruction: correlate mask image with detector plane image.

Define the “Response” of pixel x, y via

$$R(x,y) = C(x,y) - \langle C \rangle \quad (3.20)$$

where $C(x,y)$: measured count rate in detector plane, and $\langle C \rangle$ mean count rate of detector plane.

Compare $R(x,y)$ to response expected if there were a source at position α, δ on the sky using a cross correlation function

$$\mathrm{CCF}(\alpha,\delta) = \iint_{\forall x,y} R(x,y) R(\alpha,\delta;x,y)\,\mathrm{d}x\,\mathrm{d}y \quad (3.21)$$

CCF has peak if good match with real source found.

Then subtract off this source and repeat (“IROS”-method, “Iterative Removal of Sources”)

ISDC/Univ. Geneva

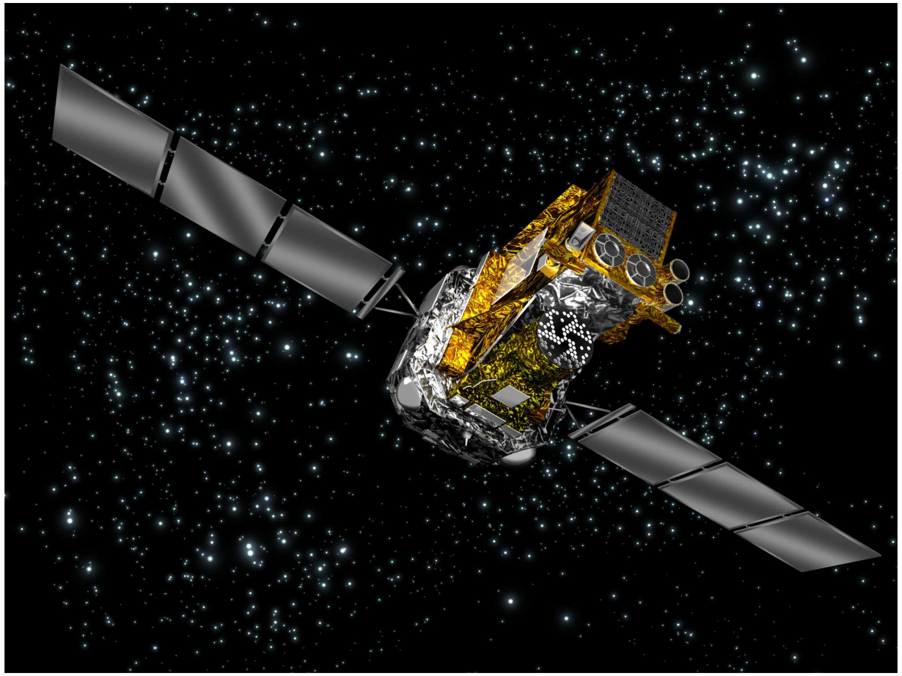

INTEGRAL: Launched 17 Oct 2002 from Baikonur on a Proton rocket.

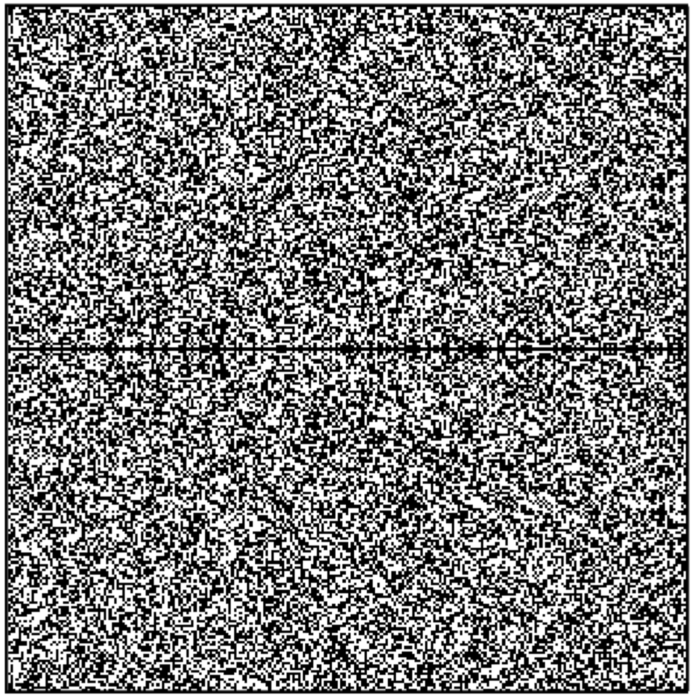

Masks can be optimized to allow source reconstruction with high signal to noise ratio.

Common buzzwords:

- Uniform Redundant Arrays (URA)
- Multiple Uniform Redundant Arrays (MURA)
- Random Masks

Mask used in COMIS-TTM experiment on *Mir*

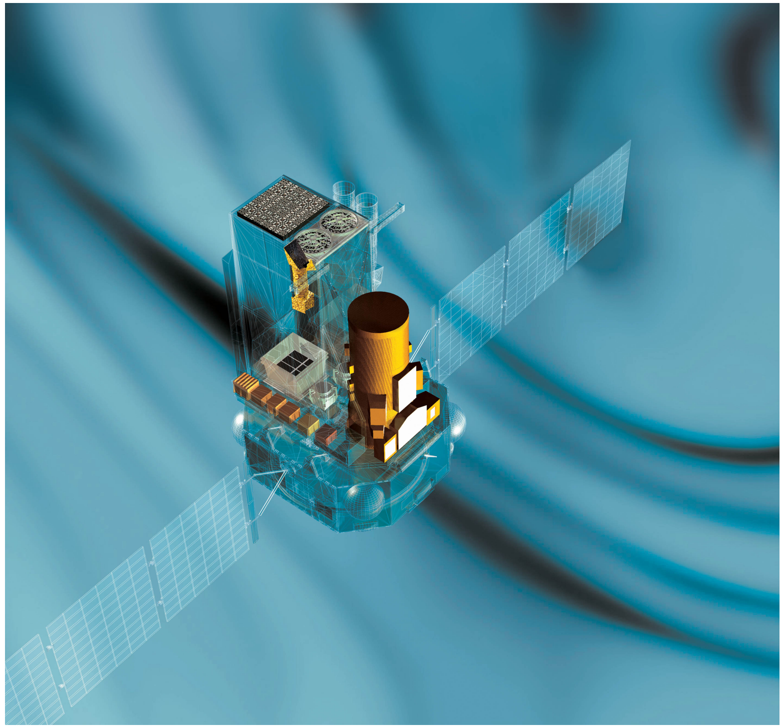

ESA

INTEGRAL: IBIS, III

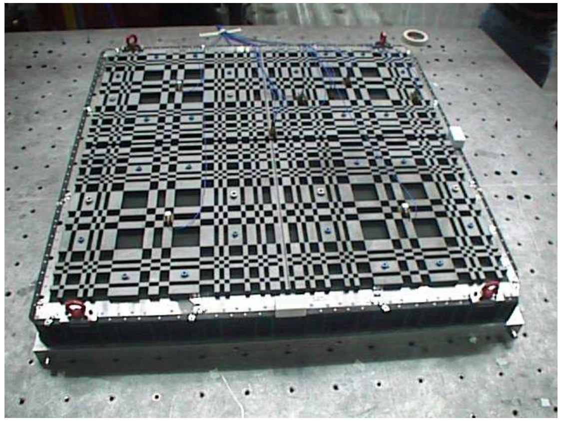

GACE/U. Valencia

IBIS: coded mask and a two-layered detector: ISGRI: CdTe solid-state detector (16000 pixels; 20 keV–few MeV) above a 4000 pixel CsI array (called PICsIT, harder energies).

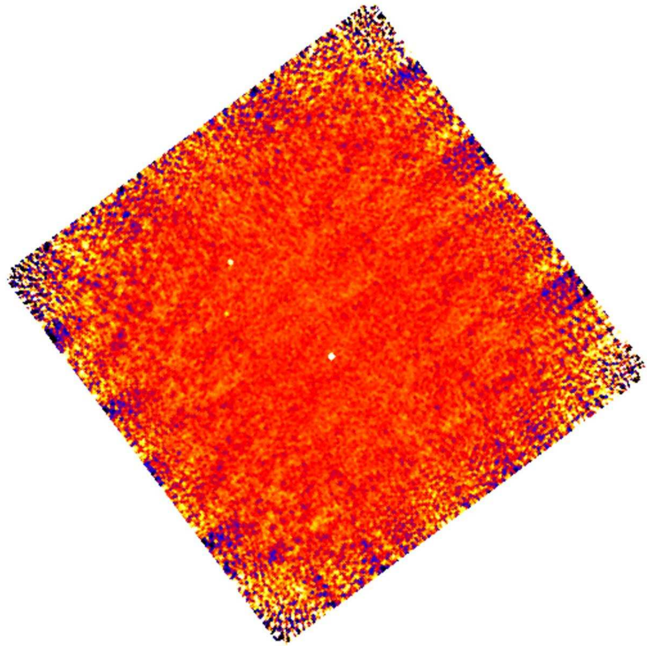

INTEGRAL: IBIS, IV

GACE/U. Valencia

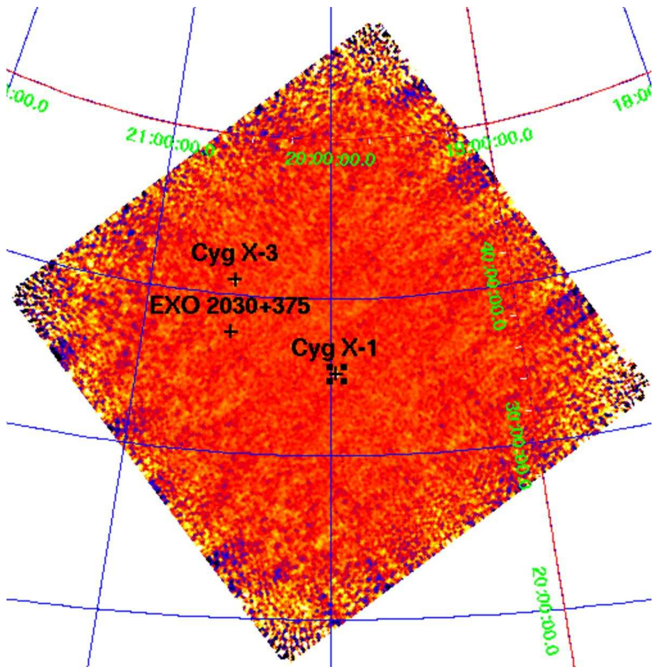

INTEGRAL: SPI

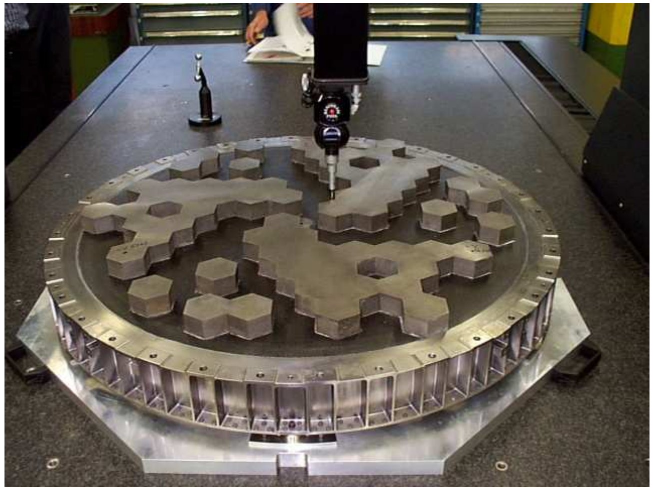

SPI: 2nd main instrument on INTEGRAL, sensitive in 20 keV–8 MeV, uses 19 Ge detectors to obtain very high resolution.
Mask: 3 cm thick tungsten, 127 hexagonal elements (63 opaque and 64 transparent), 1.7 m above the detectors; FoV: 16°, with a resolution of 2°.
Image reconstruction only possible when using multiple images ("dithering").

GACE/U. Valencia

Formal Data Analysis

Finite resolution of X-ray detectors has major implications for X-ray data analysis.

Mathematical description of the X-ray measurement process:

$$n_{\mathrm{ph}}(c) = \int_0^\infty R(c,E)\cdot A(E)\cdot F(E)\,dE \qquad (3.22)$$

where

- $n_{\mathrm{ph}}(c)$: source count rate in channel c (counts s^{-1}),
- $F(E)$: photon flux density (ph $\mathrm{cm}^2\,\mathrm{s}^{-1}\,\mathrm{keV}^{-1}$),
- $A(E)$: effective area (units: cm^2),
- $R(c,E)$: detector response (probability to detect photon of energy E in channel c).

Effective Area

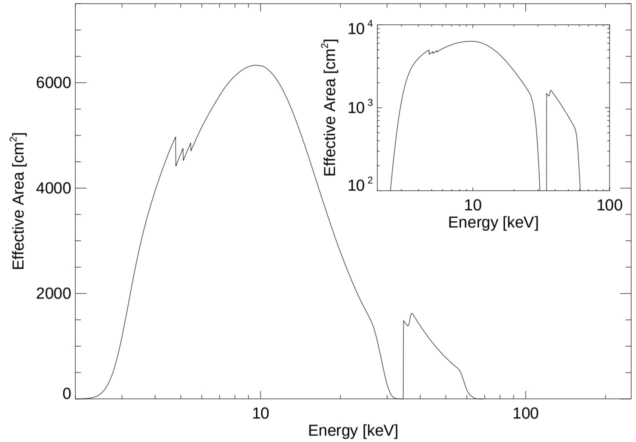

Effective Area of the Rossi X-ray Timing Explorer's Proportional Counter Array (Xe gas detector).

Response Matrix

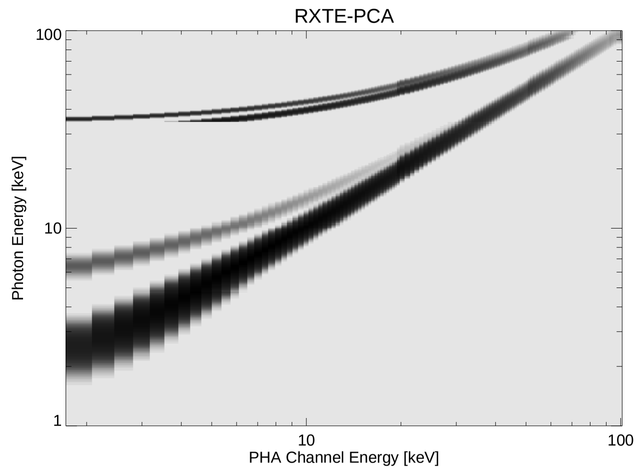

Response Matrix of the *RXTE*-PCA, log scale

Secondary "escape" peaks: response caused by Xe Kβ and Xe Lα photons escaping the detector.

χ^2-minimization

To analyze data: discretize Eq. (3.22):

$$S_{\text{ph}}(c) = \Delta T \sum_{i=0}^{n_{ch}} A(E_i) R(c,i) F(E_i) \Delta E_i \qquad (3.23)$$

where $N_{\text{ph}}(c)$: total source counts in channel c, ΔT: exposure time (s), x$A(E_i)$: effective area in energy band i ("ancilliary response file", ARF), $R(c,i)$: response matrix (RMF), $F(E_i)$: source flux in band (E_i, E_{i+i}), ΔE_i: width of energy band.

Because of background $B(c)$ (counts), what is measured is

$$N_{\text{ph}}(c) = S_{\text{ph}}(c) + B(c) \qquad (3.24)$$

So estimated source count rate is

$$\tilde{S}_{\text{ph}}(c) = N_{\text{ph}}(c) - B(c) \qquad (3.25)$$

with uncertainty (Poisson!)

$$\sigma\tilde{S}_{\text{ph}}(c) = \sqrt{\sigma N_{\text{ph}}(c)^2 + \sigma B(c)^2} = \sqrt{N_{\text{ph}}(c) + B(c)} \qquad (3.26)$$

χ^2-minimization

To get physics out of measurement, need to find $F(E_i)$.

Big problem: In general, Eq. (3.23) is *not invertible*.

$\Longrightarrow$ χ^2-minimization approach

Use a model for the source spectrum, $F(E;\boldsymbol{x})$, where $\boldsymbol{x}$ vector of parameters (e.g., source flux, power law index, absorbing column,...), and calculate predicted model counts, $M(c;\boldsymbol{x})$, using Eq. 3.23).

Then form χ^2-sum:

$$\chi^2(\boldsymbol{x}) = \sum_c \frac{\left(\tilde{S}_{\text{ph}}(c) - M(c;\boldsymbol{x})\right)^2}{\sigma\tilde{S}_{\text{ph}}(c)^2} \qquad (3.27)$$

Then vary $\boldsymbol{x}$ until χ^2 is minimal and perform statistical test based on χ^2 whether model $F(E;\boldsymbol{x})$ describes data.

Programs used: `XSPEC`, `ISIS`